PHYSICAL REVIEW D **87,** 115021 (2013)

Invisible decays of the lightest Higgs boson in supersymmetric models

B. Ananthanarayan,[1] Jayita Lahiri,[1] P. N. Pandita,[2] and Monalisa Patra[1]

[1]*Centre for High Energy Physics, Indian Institute of Science, Bangalore 560 012, India*

[2]*Department of Physics, North Eastern Hill University, Shillong 793 002, India*

(Received 15 April 2013; published 20 June 2013)

We consider supersymmetric models in which the lightest Higgs scalar can decay invisibly consistent with the constraints on the 126 GeV state discovered at the CERN LHC. We consider the invisible decay in the minimal supersymmetric standard model (MSSM), as well its extension containing an additional chiral singlet superfield, the so-called next-to-minimal or nonminimal supersymmetric standard model (NMSSM). We consider the case of MSSM with both universal as well as nonuniversal gaugino masses at the grand unified scale, and find that only an E_6 grand unified model with unnaturally large representation can give rise to sufficiently light neutralinos which can possibly lead to the invisible decay $h^0 \to \tilde{\chi}_1^0 \tilde{\chi}_1^0$. Following this, we consider the case of NMSSM in detail, where we also find that it is not possible to have the invisible decay of the lightest Higgs scalar with universal gaugino masses at the grand unified scale. We delineate the regions of the NMSSM parameter space where it is possible for the lightest Higgs boson to have a mass of about 126 GeV, and then concentrate on the region where this Higgs can decay into light neutralinos, with the soft gaugino masses M_1 and M_2 as two independent parameters, unconstrained by grand unification. We also consider, simultaneously, the other important invisible Higgs decay channel in the NMSSM, namely the decay into the lightest CP-odd scalars, $h_1 \to a_1 a_1$, which is studied in detail. With the invisible Higgs branching ratio being constrained by the present LHC results, we find that $\mu_{\rm eff} < 170$ GeV and $M_1 < 80$ GeV are disfavored in NMSSM for fixed values of the other input parameters. The dependence of our results on the parameters of NMSSM is discussed in detail.

DOI: 10.1103/PhysRevD.87.115021 PACS numbers: 14.80.Da, 14.80.Ly, 14.80.Nb

I. INTRODUCTION

There is now a possible signal for a Higgs boson at a mass of around 126 GeV from the ATLAS [1,2] and CMS [3,4] collaborations. Attention is focused on checking whether the decay widths of this particle are in accordance with the predictions of the Standard Model (SM) or its extensions, especially the supersymmetric extensions of the SM. It may, however, turn out that the SM is only a low-energy effective theory and that there are indeed particles of low masses that have evaded detection in the past due to their weak coupling to the SM particles. Candidates include such particles as the lightest neutralino in the minimal supersymmetric (MSSM) extension of the SM, and also the lightest CP-odd neutral Higgs boson of the next-to-minimal or nonminimal supersymmetric standard model (NMSSM). The Higgs sector in MSSM is extended compared to the SM and includes two Higgs doublets, H_1 and H_2, leading to five physical Higgs states, which include two CP-even Higgs bosons, h and H ($m_h < m_H$), a CP-odd Higgs, A, and a pair of charged Higgs bosons, $H^{\pm}$. The recent discovery of the Higgs-like particle (with mass $m_h \approx 126$ GeV) at the LHC requires a significant degree of fine-tuning in the parameters in the context of MSSM. This fine-tuning can be evaded in the case of the NMSSM, which is an extension of the MSSM, supplemented by a chiral singlet superfield (S). In the NMSSM, the role of the μ parameter of the MSSM is played by $\lambda\langle S\rangle$, which is generated from a trilinear superpotential coupling $\lambda H_1 H_2 S$, when S obtains a vacuum expectation value $\langle S\rangle$. This in turn leads to three CP-even Higgs bosons, $h_{1,2,3}$, two CP-odd Higgs bosons, $a_{1,2}$, and a pair of charged Higgs bosons, $H^{\pm}$. The existence of the singlet chiral superfield has implications not only for the Higgs sector, but also for the neutralino sector, where the spectrum has an additional state when compared to the neutralino sector of the MSSM. It has been found that certain regions of the parameter space of MSSM allow a Higgs boson (h) with a mass of 126 GeV, albeit with fine-tuning, satisfying the LHC results.

Since the identification of the state with a mass of 126 GeV at the LHC with the Higgs boson depends on the measurement of its couplings to different particles, it is important to study all its decay channels in the context of the SM and its supersymmetric extensions. In the allowed parameter space there are regions where the Higgs decay to the lightest neutralinos is kinematically allowed. This in turn will lead to invisible decay modes. Detailed studies have been carried out, where by assuming the discovered particle to be the SM Higgs boson, global fits have been performed to place upper bounds on its invisible decay width. The fits are performed for several cases, (a) with the assumption that the invisible Higgs width is the only new physics, and (b) with the couplings of Higgs to gluons and photons considered as free parameters, keeping the couplings to fermions and vector bosons to their SM values. We quote here the upper bounds on the invisible decay rates of the state discovered at the LHC:

(1) 28% (Ref. [5]),
(2) 61% (Ref. [6]),
(3) 69% (Refs. [7,8]),
(4) 30% (Refs. [9,10]),

consistent with the current data at a 95% confidence level. In Ref. [6], it has been pointed out that these limits can be further improved in the near future with an integrated luminosity $\mathcal{L} > 300$ fb^{-1} at $\sqrt{s} = 14$ TeV at the LHC. The discovery potential of the 7 and 8 TeV LHC in probing the invisible decaying Higgs has been studied for different final states, where the invisible Higgs is produced in association with a hard jet (from gluon fusion), two jets in the forward direction (from vector boson fusion) or the leptonic decay of Z^0 (from associated Z^0 production) [11,12]. The invisible decay width of the lightest Higgs boson has also been investigated in MSSM, taking into account the constraints obtained from the recent data [13]. Recently ATLAS [14] has looked for invisible decays of the Higgs with 4.7 fb^{-1} of 7 TeV data and 13 fb^{-1} of 8 TeV data and has placed limits on the invisible branching fraction at a 95% confidence level. They have considered the associated ZH production, with Z decaying leptonically, and have excluded invisible branching fractions greater than 65%. Being conservative, we consider the invisible branching fraction to be less than 30% in this work, as it is the most constrained value.

As mentioned above, since the Higgs and neutralino sectors of NMSSM are quite different from those of MSSM, conclusions about the invisible Higgs decay in MSSM need to be reconsidered in the context of the NMSSM, particularly in relation to the neutralino sector, as well as the additional possibility of decay into CP-odd Higgs bosons. In the light of the discovery of the SM-like Higgs boson at the LHC, considerable work has been done in the context of the Higgs sector of the NMSSM [15–21]. These studies have scanned various regions of the parameter space, mainly focusing on the regions favored by the results from LHC and the flavor physics. These studies have also considered the case where the lightest Higgs h_1 has a mass of around 100 GeV, and the second-lightest scalar h_2 is identified with the state of mass around 126 GeV observed at the LHC. This is mainly in light of the fact that with this assumption the LEP excess [22] in the $e^+e^- \to Zh \to Zb\bar{b}$ channel around $M_{b\bar{b}} \approx 100$ GeV can be explained together with the LHC data. The case with h_1 in the required mass range is also considered for constraining the NMSSM parameter space.

One of the crucial assumptions that go into limiting the parameter space of these models is the universality of the gaugino mass parameters at the grand unified scale (GUT). However, the gaugino mass parameters need not be universal at the GUT scale. If we embed the SM gauge group in a grand unified gauge group, the gaugino mass parameters can be nonuniversal at the GUT scale, thereby affecting the phenomenology of the neutralinos at the weak scale via the renormalization group evolution of these parameters. This applies to all the grand unified theories based on $SU(5)$, $SO(10)$ and E_6 grand unified theories, these being the only ones which support the chiral structure of weak interactions as observed in nature.

Depending on the gaugino masses at the GUT scale, and hence at the weak scale, the possibility of massless neutralinos has been considered in the past [23]. Such neutralinos could very well be final-state particles of the Higgs boson decay. Neutralinos lighter than half the Higgs mass have not been ruled out by current data. In the present work, we consider, among others, the decay of the lightest Higgs boson into lightest neutralinos in low-energy supersymmetric models. This includes the MSSM as well as the NMSSM. We find that it is not possible to have a massless neutralino in MSSM, not only with universal gaugino mass parameters M_1 and M_2, but even with these parameters being nonuniversal at the GUT scale, except for a higher-dimensional representation of E_6. In the case of NMSSM, although it is possible to have massless neutralinos with universal gaugino mass parameters at the GUT scale, it is not possible to obtain $m_{h_1} = 126$ GeV and simultaneously have massless neutralinos or $m_{\tilde{\chi}_1^0} \leq m_{h_1}/2$, with universal gaugino masses at the GUT scale. We relax the universality assumption on the gaugino mass parameters, with M_1 and M_2 being treated as two independent parameters, and consider the question of light neutralinos and study the decay of the lightest Higgs boson in the context of NMSSM. We find that it is possible to have a large invisible branching ratio for $h_1 \to \tilde{\chi}_1^0\tilde{\chi}_1^0$. The composition of $\tilde{\chi}_1^0$ is important in determining the invisible branching ratio. In the case of NMSSM, for certain regions of the parameter space there are additional decay channels. These mainly include the decay of h_1 to the lightest pseudoscalars, $h_1 \to a_1a_1, Z^0a_1$. These undetected channels will in turn affect the invisible branching ratio.

A very light or massless lightest neutralino which is obtained by considering M_1 and M_2 as independent parameters has to be binolike, since the LEP bound on the chargino mass has set lower limits on M_2 and μ. Since there is no lower experimental bound on this very light neutralino from collider experiments, bounds on their properties have been obtained from other sources. For instance, in Ref. [24] very light neutralinos together with R-parity violation, consistent with all the experiments, have been proposed as an explanation for the KARMEN time anomaly. Supernova 1987A data has been used to set bounds on the mass of a nearly pure binolike light neutralino ($m_{\tilde{\chi}_1^0} < 200$ MeV) in the context of MSSM [25], while gravitino cosmology with such light neutralinos has been studied in Ref. [26] by taking into account astrophysical and cosmological bounds. Moreover, a general survey on the bound of the mass of this lightest neutralino in the context of MSSM with R-parity conservation has been discussed in Ref. [27], where all the collider data along

with the contraints from cosmological observations have been considered. Overall these studies show that a very light neutralino in the context of nonuniversal gaugino masses is not ruled out by current experimental observations.

The plan of the paper is as follows: In Sec. II, we consider different patterns of gaugino masses that arise in grand unified theories based on $SU(5)$, $SO(10)$ and E_6 gauge groups. We study the existence of a massless neutralino in these theories with appropriate boundary conditions as dictated by grand unification. In Sec. III, the decay of the lightest Higgs to neutralinos is considered in the the MSSM case, with the relevant experimental constraints. The case of the invisible decay of the lightest Higgs boson for the NMSSM is considered in detail in Sec. IV. The parameter space which supports the lightest Higgs h_1 in the appropriate mass window 123–127 GeV is explored. In this section we also consider the decay of the lightest Higgs boson to the lightest CP-odd Higgs. Finally, we summarize our results in Sec. V. In the Appendix, we briefly summarize some of the details regarding nonuniversal gaugino masses in GUTS.

II. MINIMAL SUPERSYMMETRIC STANDARD MODEL WITH GUT BOUNDARY CONDITIONS

We begin our analysis with a brief review of the existence of a massless or a light neutralino in the minimal supersymmetric standard model. We recall that the neutralinos are an admixture of the fermionic partners of the two Higgs doublets, H_1 and H_2, and the fermionic partners of the neutral gauge bosons. When the electroweak symmetry is broken, the physical mass eigenstates are obtained from the diagonalization of the neutralino mass matrix [28,29]

$$M_{\rm MSSM} = \begin{pmatrix} M_1 & 0 & -m_Z \sin\theta_W \cos\beta & m_Z \sin\theta_W \sin\beta \\ 0 & M_2 & m_Z \cos\theta_W \cos\beta & -m_Z \cos\theta_W \sin\beta \\ -m_Z \sin\theta_W \cos\beta & m_Z \cos\theta_W \cos\beta & 0 & -\mu \\ m_Z \sin\theta_W \sin\beta & -m_Z \cos\theta_W \sin\beta & -\mu & 0 \end{pmatrix}, \tag{2.1}$$

where M_1 and M_2 are the $U(1)_Y$ and the $SU(2)_L$ soft supersymmetry breaking gaugino mass parameters, μ is the Higgs(ino) mass parameter, m_Z is the Z boson mass, θ_W is the weak mixing angle, and $\tan\beta = v_2/v_1$ is the ratio of the vacuum expectation values of the neutral components of the two Higgs doublet fields H_1 and H_2. We are interested in finding a light neutralino eigenstate of the neutralino mass matrix [Eq. (2.1)]. For this purpose we consider the limiting case of the massless neutralino, which, at the tree level, arises when the determinant of the matrix (2.1) is zero. This leads to the condition [23]

$$\mu[m_Z^2 \sin 2\beta(M_1 \cos^2\theta_W + M_2 \sin^2\theta_W) - M_1 M_2] = 0. \tag{2.2}$$

The solution with $\mu = 0$ is excluded by the lower bounds on the chargino mass from the LEP experiments [30], which impose the constraint

$$|\mu|, \qquad M_2 \geq 100 \text{ GeV}. \tag{2.3}$$

The other possible solution to Eq. (2.2) can be written as

$$M_1 = \frac{M_2 m_Z^2 \sin^2\theta_W \sin 2\beta}{\mu M_2 - m_Z^2 \cos^2\theta_W \sin 2\beta}. \tag{2.4}$$

Therefore, with fixed values of μ, M_2 and $\tan\beta$, for a massless neutralino, one must find a value of M_1 consistent with Eq. (2.4). The condition (2.4) can be expressed in terms of $r \equiv M_1/M_2$, so as to check whether a massless neutralino is allowed in the MSSM. In terms of r, the condition (2.4) can be written as

$$\mu M_2 = \frac{m_Z^2}{r} \sin 2\beta(\sin^2\theta_W + r\cos^2\theta_W), \tag{2.5}$$

which must be satisfied, consistent with the experimental constraints of Eq. (2.3), in order to have a massless neutralino.

It is known that the condition (2.5) is not satisfied in MSSM with universal gaugino masses at the grand unified scale [23]. In the next subsection, we briefly recall this and then proceed to study whether this condition can be satisfied in MSSM with nonuniversal boundary conditions on the gaugino mass parameters at the grand unified scale.

A. Gaugino masses in grand unified theories

In the MSSM, with universal gaugino masses at the grand unified scale, usually referred to as mSUGRA, the soft supersymmetry breaking gaugino mass parameters M_1, M_2, and M_3 satisfy the boundary condition

$$M_1 = M_2 = M_3 = m_{1/2} \tag{2.6}$$

at the grand unified scale M_G. Furthermore, the three gauge couplings corresponding to the gauge groups $U(1)_Y$, $SU(2)_L$ and $SU(3)_C$ satisfy ($\alpha_i = g_i^2/4\pi$, $i = 1, 2, 3$)

$$\alpha_1 = \alpha_2 = \alpha_3 = \alpha_G \tag{2.7}$$

at the GUT scale M_G. Using the one-loop renormalization group equations [31] for the gaugino masses and the gauge couplings, this leads to the ratio

$$M_1 : M_2 : M_3 \simeq 1 : 2 : 7.1 \tag{2.8}$$

for the soft gaugino masses at the electroweak scale m_Z. In the following, for definiteness, we shall consider the value of $\tan\beta = 10$. From Eq. (2.8), we see that the value of r is 0.5. Using this in Eq. (2.5), we conclude that either $\mu \approx M_2 \approx m_Z$, or $\mu \gg m_Z$ and $M_2 \ll m_Z$, or $\mu \ll m_Z$ and $M_2 \gg m_Z$. None of these conditions are consistent with the LEP constraint of Eq. (2.3). Thus, a massless neutralino is excluded in the case of MSSM with universal gaugino masses at the GUT scale.

We recall here that universal soft supersymmetry breaking gaugino masses are not the only possibility in a grand unified theory. In fact, nonuniversal boundary conditions for the soft gaugino masses can naturally arise in a grand unified supersymmetric theory. It is, therefore, important to study whether it is possible to have a light neutralino with nonuniversal boundary conditions at the grand unified scale. To this end, we recall the essential features of the boundary conditions on the gaugino masses in a grand unified theory.

B. Nonuniversal gaugino masses in grand unified theories

We now consider the neutralino masses and mixing in the minimal supersymmetric standard model with nonuniversal boundary conditions at the GUT scale, which arise in $SU(5)$, $SO(10)$ and E_6 grand unified theories. As discussed in Sec. II A, in the simplest supersymmetric model with universal gaugino masses, $M_i (i = 1, 2, 3)$ are taken to be equal at the grand unified scale. However, in supersymmetric theories with an underlying grand unified gauge group, the gaugino masses need not necessarily be equal at the GUT scale.

In the Appendix, we recall the essential features of the embedding of the SM gauge group in different grand unified gauge groups, namely $SU(5)$, $SO(10)$ and E_6, these being the only ones which support the chiral structure of weak interactions as observed in nature [32]. The gaugino mass parameters for the different representations that arise in the symmetric product of the adjoint representations of the respective gauge groups are shown in Tables IV, V, VI, VII, and VIII of the Appendix. Using the value of the ratio r at the electroweak scale from the respective tables, and following the same procedure as in the case of MSSM with universal gaugino masses in the previous subsection, we see from Eq. (2.5) and Tables IV, V, VI, and VII that none of the representations of $SU(5)$ and $SO(10)$ can have a massless neutralino in the light of the experimental constraints of Eq. (2.3). We also find that in the case of E_6, for all the representations except one, there can be no massless neutralino which satisfies the condition of Eq. (2.5). Only the higher-dimensional **2430** representation of E_6, as shown in Tables X and XI, with the **770** dimensional representation of $SO(10)$ and a singlet of $SU(4)'$, allows the possibility of a light neutralino consistent with the phenomenological constraint of Eq. (2.3). We shall not consider this possibility any further in this paper.

III. DECAY OF HIGGS TO NEUTRALINOS IN THE MSSM

In the previous section, we have seen that in MSSM with universal gaugino mass parameters at the GUT scale, with $r = 0.5$ at the weak scale, it is not possible to obtain a massless neutralino. Since $r \leq 0.04$ for a massless neutralino, it is not possible to obtain a massless neutralino in a GUT even with nonuniversal gaugino masses M_i at the GUT scale. The only possible exception is the higher-dimensional representation **2430** of E_6, with $r = 0.02$, and this is not an appealing possibility. Thus, in order to obtain a massless neutralino, we must consider arbitrary gaugino masses in the MSSM. If the neutralino is sufficiently light, then the invisible decay $h^0 \to \tilde{\chi}_1^0 \tilde{\chi}_1^0$ will be kinematically allowed in MSSM.

Recalling that in the MSSM, the decay width of the lightest Higgs boson to a pair of lightest neutralinos can be written as [33]

$$\Gamma(h^0 \to \tilde{\chi}_1^0 \tilde{\chi}_1^0) = \frac{G_F m_W^2 m_h}{2\sqrt{2}\pi}(1 - 4m_{\tilde{\chi}_1^0}^2/m_h^2)^{3/2} \times [(Z_{12} - \tan\theta_W Z_{11}) \times (Z_{13}\sin\alpha + Z_{14}\cos\alpha)]^2, \quad (3.1)$$

where Z_{ij} are the elements of the matrix Z which diagonalizes the neutralino mass matrix, and α is the mixing angle in the CP-even Higgs sector. In the decoupling limit, when the mass m_A of the pseudoscalar Higgs boson is large compared to the Z boson mass m_Z, with $\alpha \to \beta - \pi/2$, the decay width [Eq. (3.1)] can be written as [13]

$$\Gamma(h^0 \to \tilde{\chi}_1^0 \tilde{\chi}_1^0) = \frac{G_F m_W^2 m_h}{2\sqrt{2}\pi}(1 - 4m_{\tilde{\chi}_1^0}^2/m_h^2)^{3/2} \times [(Z_{12} - \tan\theta_W Z_{11}) \times (Z_{14}\sin\beta - Z_{13}\cos\beta)]^2. \quad (3.2)$$

The composition of the lightest neutralino $\tilde{\chi}_1^0$ in terms of the gauginos and Higgsinos can be written as [23,34]

$$\tilde{\chi}_1^0 = Z_{11}\tilde{B} + Z_{12}\tilde{W}^3 + Z_{13}\tilde{H}_1^0 + Z_{14}\tilde{H}_2^0, \quad (3.3)$$

where

$$Z_{1i} = \left(1, -\frac{1}{2}\frac{m_Z^2 \sin 2\theta_W \sin 2\beta}{\mu M_2 - m_Z^2 \cos^2\theta_W \sin 2\beta}, \frac{m_Z M_2 \sin\theta_W \sin\beta}{\mu M_2 - m_Z^2 \cos^2\theta_W \sin 2\beta}, \frac{m_Z M_2 \sin\theta_W \cos\beta}{\mu M_2 - m_Z^2 \cos^2\theta_W \sin 2\beta}\right). \quad (3.4)$$

The invisible decay of the lightest Higgs boson to the lightest neutralinos, if kinematically allowed, is mainly constrained by the Z invisible decay rate. This invisible decay width has been measured very precisely by the LEP experiments [30] with

$$\Gamma(Z^0 \to \tilde{\chi}_1^0 \tilde{\chi}_1^0) < 3 \text{ MeV}. \tag{3.5}$$

The Z width to a pair of lightest neutralinos can be written as [35]

$$\Gamma(Z^0 \to \tilde{\chi}_1^0 \tilde{\chi}_1^0) = \frac{G_F m_Z^3}{6\sqrt{2}\pi}(Z_{13}^2 - Z_{14}^2)\left(1 - \frac{4m_{\tilde{\chi}_1^0}^2}{m_{Z^0}^2}\right)^{3/2}. \tag{3.6}$$

For our analysis we have used the program CalcHEP [36], with $\tan\beta = 10$. The trilinear soft supersymmetry breaking coupling A_t has been adjusted in order to obtain a lightest Higgs boson of mass ≈ 126 GeV. The gluino mass is taken to be 1400 GeV [37], and the squarks are assumed to have a mass above 1 TeV [38], thereby respecting the current experimental bounds. We have presented our results for a fixed value of M_2, with the parameters μ and M_1 being varied. Since the results do not change significantly as a function of M_2, only a particular value of M_2 is considered. In Fig. 1 we show the contour plots of the constant lightest neutralino mass in MSSM, and in Fig. 2 we show the corresponding contours of the constant invisible branching ratio of the lightest Higgs boson. In our calculations we have imposed the constraint of the lightest chargino mass bound $m_{\tilde{\chi}^+} > 94$ GeV from the LEP experiments as well as the bound from the invisible Z^0-decay width coming from Z^0 decay into neutralinos. Our results agree with those of Ref. [13]. This sets the stage for our analysis of the invisible decay of the lightest Higgs boson in the NMSSM, which we carry out in the next section.

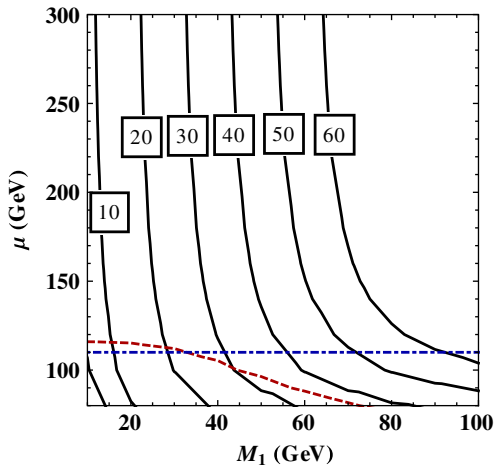

FIG. 1 (color online). The contours of constant lightest neutralino mass in MSSM in the $\mu - M_1$ plane for $\tan\beta = 10$ and $M_2 = 200$ GeV.

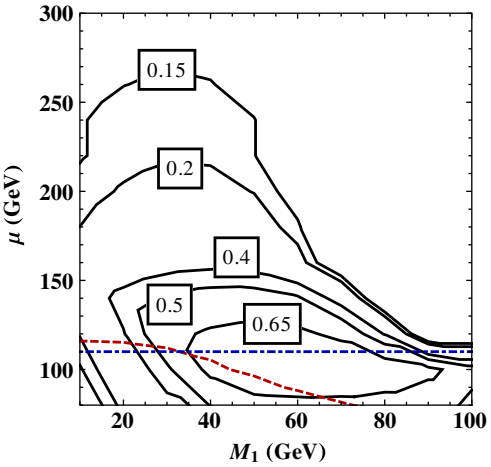

FIG. 2 (color online). The contours of constant branching ratio of $(h \to \tilde{\chi}_1^0 \tilde{\chi}_1^0)$ in MSSM for a fixed value of $\tan\beta = 10$ and $M_2 = 200$ GeV.

IV. DECAY OF THE LIGHTEST HIGGS TO NEUTRALINOS AND PSEUDOSCALARS IN THE NMSSM

The NMSSM is characterized by the presence of the gauge singlet superfields S in addition to the two Higgs doublets H_1 and H_2 of the minimal supersymmetric standard model. The Higgs(ino) mass term $\mu H_1 H_2$ in the superpotential of the MSSM is replaced by the trilinear coupling $\lambda S H_1 H_2$, where λ is a dimensionless coupling [39–45]. In addition, there is also a trilinear self-coupling of the singlet, namely S^3. The part of the superpotential involving only the Higgs superfields has the form

$$W_{\text{NMSSM}} = \lambda S H_1 H_2 - \frac{\kappa}{3} S^3. \tag{4.1}$$

After the electroweak symmetry breaking, the vacuum expectation value (VEV) of the singlet field, $\langle S \rangle \equiv x$, generates an effective μ parameter, $\mu_{\text{eff}} = \lambda x$, which is naturally of the order of the electroweak scale, thus providing a solution to the μ problem of the MSSM. Thus, compared to the two independent parameters in the Higgs sector of the MSSM at tree level ($\tan\beta$, M_A), the Higgs sector of NMSSM is described by six parameters—μ_{eff}, λ, κ, $\tan\beta$, A_λ and A_κ—where A_λ and A_κ are the trilinear supersymmetry breaking couplings.

Because of the addition of the singlet, the neutralino mass matrix in NMSSM is a 5×5 matrix, which in the bino, wino, Higgsino and singlino basis can be written as [46–48]

$$M_{\rm NMSSM} = \begin{pmatrix} M_1 & 0 & -m_Z \sin\theta_W \cos\beta & m_Z \sin\theta_W \sin\beta & 0 \\ 0 & M_2 & m_Z \cos\theta_W \cos\beta & -m_Z \cos\theta_W \sin\beta & 0 \\ -m_Z \sin\theta_W \cos\beta & m_Z \cos\theta_W \cos\beta & 0 & -\mu_{\rm eff} & -\lambda v_2 \\ m_Z \sin\theta_W \sin\beta & -m_Z \cos\theta_W \sin\beta & -\mu_{\rm eff} & 0 & -\lambda v_1 \\ 0 & 0 & -\lambda v_2 & -\lambda v_1 & 2\kappa x \end{pmatrix}. \quad (4.2)$$

The neutralino sector in this case is described by six parameters: $\mu_{\rm eff}$, M_1, M_2, $\tan\beta$, λ and κ. For a massless neutralino, the determinant of the mass matrix [Eq. (4.2)] should be zero, which leads to [23]

$$2\kappa x \mu_{\rm eff}(\Delta_0 \sin 2\beta - \mu_{\rm eff} M_1 M_2) + \lambda^2 v^2[\Delta_0 - \mu_{\rm eff} M_1 M_2 \sin 2\beta] = 0, \quad (4.3)$$

where $\Delta_0 = m_Z^2(M_1 \cos^2\theta_W + M_2 \sin^2\theta_W)$. Equation (4.3) in turn leads to the following condition:

$$\kappa = \frac{\lambda}{2}\left(\frac{\lambda v}{\mu_{\rm eff}}\right)^2 \frac{\Delta_0 - \mu_{\rm eff} M_1 M_2 \sin 2\beta}{\mu_{\rm eff} M_1 M_2 - \Delta_0 \sin 2\beta} \quad (4.4)$$

for a massless neutralino in the NMSSM. The composition of the lightest neutralino $\tilde{\chi}_1^0$ in terms of the gauginos, Higgsinos and the singlino is in turn given by

$$\tilde{\chi}_1^0 = Z'_{11}\tilde{B} + Z'_{12}\tilde{W}^3 + Z'_{13}\tilde{H}_1^0 + Z'_{14}\tilde{H}_2^0 + Z'_{15}S, \quad (4.5)$$

where

$$Z'_{1i} = \left(-\frac{\lambda v m_Z \cos 2\beta \sin\theta_W M_2}{\Delta_1}, \frac{\lambda v m_Z \cos 2\beta \cos\theta_W M_1}{\Delta_1}, \frac{v(\sin\beta\Delta_0 - \mu_{\rm eff} M_1 M_2 \cos\beta)}{x\Delta_1}, \frac{v(\cos\beta\Delta_0 - \mu_{\rm eff} M_1 M_2 \sin\beta)}{x\Delta_1}, 1\right) \quad (4.6)$$

and $\Delta_1 = \mu_{\rm eff} M_1 M_2 - \Delta_0 \sin 2\beta$. Here Z' is the matrix which diagonalizes the 5×5 neutralino mass matrix of the NMSSM. As in the case of MSSM, we have assumed CP conservation in the neutralino sector in our analysis.

We have performed our analysis for the NMSSM with the set of relevant parameters varied in the following ranges:

(1) $4 \leq \tan\beta \leq 11$, 100 GeV $\leq \mu_{\rm eff} \leq$ 200 GeV,
(2) $0.55 \leq \lambda \leq 0.7$, $0.33 \leq \kappa \leq 0.8$,
(3) -10 GeV $\leq A_\kappa \leq$ 10 GeV, 500 GeV $\leq A_\lambda \leq$ 1000 GeV.

This range is considered because we are mainly interested in the region where the lightest CP-even Higgs (h_1) of the NMSSM will lead to a SM-like Higgs in the mass range 124 GeV $\leq m_{h_1} \leq$ 127 GeV. We have restricted ourselves to small values of $\tan\beta$, since it is difficult to get a SM-like lightest Higgs in the mass window of 124–127 GeV with larger values of $\tan\beta$. The range for λ and κ are chosen by imposing the theoretical constraint that there are no charge- and color-breaking global minima of the scalar potential, and that a Landau pole does not develop below the GUT scale. We are interested mainly in relatively large values of λ, so as to increase the tree-level mass of the CP-even Higgs boson, leading naturally to a SM-like Higgs boson. This in turn implies a large doublet singlet mixing in the Higgs sector. The lightest Higgs boson with mass $\approx$ 126 GeV can also be achieved in NMSSM, as in MSSM through loop level corrections coming from stop, with large values of A_t. In this case λ can be small ($\lambda \approx 0.1$), typically preferred for negative values of A_κ. Here we have considered the former case, where the Higgs mass is obtained naturally at tree level. Since we are mainly interested in large λ, the other NMSSM parameters are considered accordingly so as to satisfy the constraints from precision electroweak measurements; see Ref. [49]. In addition, we have also taken into account the latest experimental constraints from the LHC on the gluino and other sparticle masses. The gluino mass is chosen above 1400 GeV, and the squark masses are set to 1 TeV or more, as in the MSSM analysis. Additional constraints from B physics and the anomalous magnetic moment of the muon are taken into account using CalcHEP, which has the built-in NMSSMTools package [50,51]. In Table I we summarize the values of the various input parameters used for our analysis. Considering the relation between M_1, M_2 and M_3, we choose the $SU(3)_C$ gaugino mass parameter $M_3 =$ 1402 GeV, with the remaining two soft SUSY breaking gaugino parameters having values $M_1 =$ 197 GeV and $M_2 =$ 395 GeV, respectively. With this, and using Eq. (4.4), we find that it is not possible to get a massless neutralino in the NMSSM with $m_{h_1} \approx$ 126 GeV. We arrive at this conclusion by taking into account the experimental constraint in Eq. (2.3). This result holds in the entire parameter space considered in our analyses. If the condition $m_{h_1} \approx 126$ GeV is relaxed with the mass of the next-to-lightest CP-even Higgs m_{h_2} to be in the mass range 124–127 GeV, then it is possible to obtain a massless neutralino. We do not consider this possibility here. Thus, for NMSSM, in the region of the parameter space considered by us, universal boundary conditions on the gaugino masses at the GUT scale cannot lead to a decay for $h_1 \to \tilde{\chi}_1^0\tilde{\chi}_1^0$, since

TABLE I. Input parameters for the NMSSM.

$\tan\beta = 10$	$\mu_{\rm eff} = 130$ GeV	$A_\lambda = 880$ GeV	$A_\kappa = 10$ GeV
$M_3 = 1402$ GeV	$A_t = 2800$ GeV	$A_b = 2800$ GeV	$A_\tau = 1000$ GeV

TABLE II. The mass of the lightest CP-even Higgs h_1, the lightest neutralino $\tilde{\chi}_1^0$ and the lightest CP-odd pseudoscalar Higgs a_1 in the NMSSM with universal gaugino masses at the GUT scale, for the parameter space considered in Table I and with $M_1 = 197$ GeV, $M_2 = 395$ GeV.

	$\kappa = 0.33$			$\kappa = 0.43$			$\kappa = 0.53$			$\kappa = 0.63$			$\kappa = 0.73$		
λ	m_{h_1}	$m_{\tilde{\chi}_1^0}$	m_{a_1}	m_{h_1}	$m_{\tilde{\chi}_1^0}$	m_{a_1}	m_{h_1}	$m_{\tilde{\chi}_1^0}$	m_{a_1}	m_{h_1}	$m_{\tilde{\chi}_1^0}$	m_{a_1}	m_{h_1}	$m_{\tilde{\chi}_1^0}$	m_{a_1}
0.55	113	73.7	46.1	122	82.9	51.4	125	88.7	55.7	125.6	92.5	59.2	126	95.1	62.2
0.58	108.3	69.5	50	120	79.1	55.9	124	85.5	60.9	125	89.8	65	126	92.8	68.6
0.61	102.6	65.4	53.5	117.9	75.4	60	123	82.2	65.5	124.9	86.9	70.1	125.8	90.4	74.2
0.64	96.4	61.4	56.7	114.9	71.6	63.8	121.7	78.8	69.7	124.3	83.9	74.8	125.5	87.7	79.2
0.67	89.8	57.5	59.7	111.1	67.8	67.2	119.9	75.3	73.5	123.4	80.9	79.1	125	84.9	83.9
0.7	82.7	53.9	62.4	106.5	64.1	70.3	117.7	71.9	77.1	122	77.7	82.9	124	82.1	88.2

$m_{\tilde{\chi}_1^0} \geq m_{h_1}/2$ in this region, i.e., the decay is not kinematically possible. This can be seen from Table II, where we present the values of m_{h_1}, $m_{\tilde{\chi}_1^0}$ and m_{a_1} for different combinations of λ and κ. The other parameters are fixed, with the values considered in Table I. It can be easily seen from Table II that for the mass of m_{h_1} around 126 GeV, the lightest neutralino mass varies in the range 80–90 GeV. Therefore, the invisible decay to the lightest neutralinos is not kinematically allowed. This result is also true, when λ is small, as discussed before, for the case where the lighest Higgs achieves mass through loop corrections. We have found $m_{\tilde{\chi}_1^0} \geq m_{h_1}/2$ by scanning the entire parameter (λ, κ) space with $0.001 \leq \lambda \leq 0.7$ and $0.001 \leq \kappa \leq 0.8$. The dependence of our results on the other input parameters which were fixed for this analysis will be discussed below.

It may be noted that in the case of the NMSSM, the lightest neutralino has a singlino component along with the gaugino and Higgsino components. We have analysed the singlino component of $\tilde{\chi}_1^0$ in the parameter space λ and κ, with the other parameters fixed at the values as in Table I, and with $M_1 = 197$ GeV, $M_2 = 395$ GeV. The gaugino-plus-Higgsino and the singlino components are, respectively, given by $Z'^2_{11} + Z'^2_{12}$, $Z'^2_{13} + Z'^2_{14}$, and Z'^2_{15}. The decay width of h_1 to the lightest neutralino in NMSSM can be written as [52,53]

$$\Gamma(h_1 \to \chi_1^0 \chi_1^0) = \frac{m_{h_1}}{16\pi}(1 - 4m^2_{\chi_1^0}/m^2_{s_1})^{3/2} Q'^{L^2}_{111}, \quad (4.7)$$

$$\begin{aligned} Q'_{111} = \Big[& \frac{g}{c_W} Z'_{12}((U^s_{11}\cos\beta + U^s_{12}\sin\beta)Z'_{13} \\ & + (U^s_{11}\sin\beta - U^s_{12}\cos\beta)Z'_{14}) \\ & + \sqrt{2}\lambda Z'_{15}(U^s_{11}\cos\beta + U^s_{12}\sin\beta)Z'_{14} \\ & - (U^s_{11}\sin\beta - U^s_{12}\cos\beta)Z'_{13}) \Big] \\ & - 2\sqrt{2}\kappa U^s_{13}|Z'_{15}|^2, \end{aligned} \quad (4.8)$$

where U^s is the matrix that diagonalizes the 3×3 scalar Higgs mass matrix of the NMSSM. It is clear from Eq. (4.8) that as the singlino contribution appears with a negative sign in the decay width, the invisible decay width of h_1 would decrease as the singlino composition increases. Nevertheless, no simple explanation is available, since in practice either sign solutions for the singlino matrix element can be found. We show in Fig. 3 the contours of a constant singlino component in the case with universal gaugino masses at the GUT scale, where we see that there is a significant singlino component in the lightest neutralino. For lower values of M_1, the lightest neutralino has a dominant gaugino component. Since in this case M_1 is around 180 GeV, due to the constraint on the gluino mass, the gaugino and Higgsino components decrease, with the neutralino being dominantly a singlino.

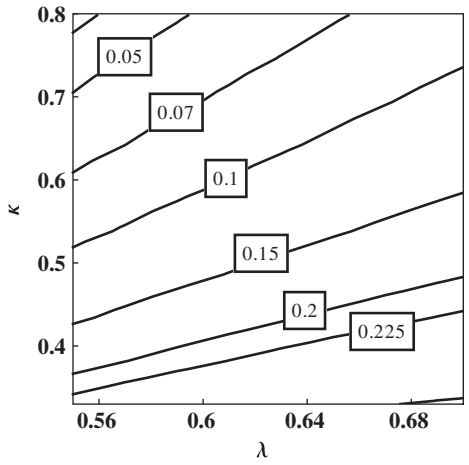

FIG. 3. Contours of constant singlino composition $|Z'_{15}|^2$ in the $\kappa - \lambda$ plane for NMSSM, with universal gaugino masses at the GUT scale with fixed values of $M_1 = 197$ GeV, $M_2 = 395$ GeV, and the other input parameters as given in Table I.

TABLE III. The relic density of the lightest neutralino, for different values of M_1, for the parameter space considered in Table I and with $M_2 = 200$ GeV.

	M_1 (GeV)														
	$\kappa = 0.33$			$\kappa = 0.43$			$\kappa = 0.53$			$\kappa = 0.63$			$\kappa = 0.73$		
λ	20	50	80	20	50	80	20	50	80	20	50	80	20	50	80
0.55	4.67	0.33	0.02	3.08	0.21	0.04	2.43	0.13	0.03	2.1	0.10	0.01	1.89	0.08	0.01
0.58	6.33	0.14	0.34	3.77	0.16	0.04	2.83	0.13	0.05	2.36	0.09	0.05	2.09	0.06	0.04
0.61	9.13	$\approx 10^{-4}$	0.13	4.80	$\approx 10^{-4}$	0.02	3.37	$\approx 10^{-4}$	0.05	2.71	$\approx 10^{-3}$	0.06	2.34	$\approx 10^{-2}$	0.06
0.64	14.3	0.05	0.11	6.40	0.02	0.31	4.15	0.03	0.02	3.17	0.07	0.05	2.65	0.11	0.06
0.67	25.8	0.44	0.05	9.01	0.42	0.08	5.29	0.40	0.03	3.83	0.33	0.04	3.09	0.24	0.05
0.7	68.3	0.68	$\approx 10^{-5}$	13.65	0.79	0.02	70.57	0.73	0.06	4.76	0.51	0.01	3.67	0.34	0.03

Here it is important to consider the possibility that our parameter choice could lead to overclosure of the universe. We use MicroOmegas [54,55] implemented in NMSSMTools to compute the dark matter relic density of the lightest neutralino, $\tilde{\chi}_1^0$. We show in Table III the corresponding relic density for different values of M_1, in the $\kappa - \lambda$ parameter space. The measurements from WMAP have constrained the relic density of dark matter [56], i.e., $(0.0925 < \Omega h^2 < 0.1287)$. It can be seen from the table that the relic density constrains most of the $(\lambda - \kappa)$ parameter space, depending on the value of M_1. When the lightest neutralino is mostly a bino, due to a small value of M_1, the relic density is sufficiently large at smaller values of κ and larger values of λ. This has to do with the dependence of neutralino mass on λ and κ, which will be discussed later. The relic density mostly constrains smaller values of $M_1 < 50$ GeV, and as will be seen later, this region is disfavored by the Higgs invisible branching ratio. Thus we see that our choice does not come in conflict with the cosmological relic density constraint.

With the universal gaugino masses at the GUT scale, the Higgs invisible decay to the lightest neutralinos is kinematically not allowed in the NMSSM. We, therefore, use M_1 and M_2 as two independent parameters. Before proceeding further, we would like to comment on the dependence of our results on the various input parameters considered in our analysis. For this we consider the dependence of the mass of the lightest CP-even Higgs h_1, the lightest pseudoscalar Higgs a_1 and the lightest neutralino $\tilde{\chi}_1^0$ on different NMSSM parameters: μ_{eff}, λ, κ, $\tan\beta$, A_λ and A_κ. We consider the mass of the lightest pseudoscalar Higgs because for certain regions of the parameter space it is rather light—in fact, a_1 can be lighter than h_1. This could lead to additional decay channels for the lightest CP-even Higgs, mainly the channel $h_1 \to a_1 a_1$, and $h_1 \to a_1 Z^0$. In the observed mass window of the Higgs, the decay to $b\bar{b}$ is dominant, but with the additional decay channel $h_1 \to a_1 a_1$ and $a_1 \to b\bar{b}$, $\tau\bar{\tau}$, $\mu\bar{\mu}$, $\tilde{\chi}_1^0\tilde{\chi}_1^0$, depending on the mass of the lightest pseudoscalar, the branching fraction $h_1 \to b\bar{b}$ can be significantly reduced. It may be emphasized that the LHC sensitivity in case of Higgs decay to light pseudoscalars depends on the decay mode of the pseudoscalars. For the parameter space considered in our analyses, a_1 mainly decays to $b\bar{b}$. At the LHC, this channel will be dominated by a large QCD background. The $b\bar{b}$ channel in the Higgs decay has been searched for at the LHC, and indicates a weak SM Higgs signal of around 1–2σ. This particular decay channel of h_1 decaying to pseudoscalar a_1 pairs has also been discussed in Refs. [57–62].

Most of the studies in the context of the lightest pseudoscalar have been carried out in the light of the LEP constraints on the Higgs mass, $m_h > 114$ GeV, along with the LEP excess for a lighter Higgs around 100 GeV, through $Z^0 h$ production, where h decays primarily to b quarks. It has been concluded that if in the NMSSM, the Higgs boson decays mainly into a_1 pairs, and with $m_{a_1} < 2m_b$, then the LEP constraints can be evaded. It will be possible to have a lighter Higgs of mass less than 105 GeV, satisfying all precision electroweak results. This is often referred to as the "ideal" Higgs boson scenario. The *BABAR* [63] and Belle [64] experiments have placed limits on m_{a_1}, using the data collected at the Υ resonances, but it is based on the "ideal" Higgs boson scenario. Since in our case the lightest Higgs is around 126 GeV, the constraints above on m_{a_1} do not hold. In addition, the LHC experiments [65,66] have also performed a search for a low-mass pseudoscalar a_1, with a_1 decaying to two muons, and have obtained the best experimental limits to date.

In Figs. 4–9, we show the dependence of the mass of h_1, a_1, $\tilde{\chi}_1^0$ on various parameters of NMSSM. While displaying the dependence on a particular parameter, the other parameters are kept fixed at their values in Table I, with λ and κ fixed to the lowest acceptable values of 0.55 and 0.33, respectively. We have fixed the value of the soft gaugino mass parameter $M_2 = 200$ GeV, with $M_1 = 120$ GeV. Since the mass m_{h_1} of CP-even, and the mass m_{a_1} of the pseudoscalar Higgs are independent of the soft gaugino mass parameters, the dependence of their mass on various input parameters is independent of the universal gaugino masses at the GUT scale. The mass of the lightest neutralino being sensitive to gaugino masses can be scaled up and down, with its mass as low as 1 GeV for $M_1 = 5$ GeV. It is seen from Figs. 4 and 5 that m_{h_1} and m_{a_1} are sensitive to

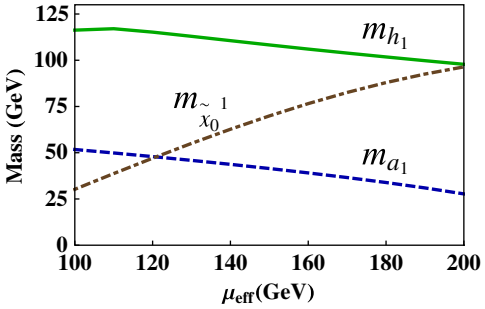

FIG. 4 (color online). Dependence of m_{h_1} (green solid line), m_{a_1} (blue dashed line) and $m_{\tilde{\chi}_1^0}$ (brown dot-dashed line) on $\mu_{\rm eff}$, for $M_1 = 120$ GeV, $M_2 = 200$ GeV, $\lambda = 0.55$ and $\kappa = 0.33$ with the other input parameters fixed to the values given in Table I.

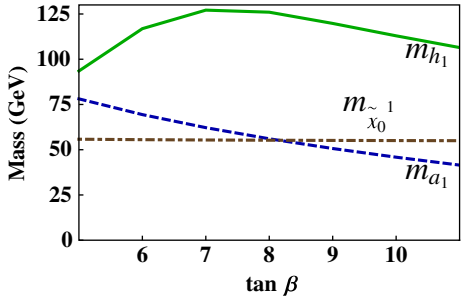

FIG. 5 (color online). Dependence of m_{h_1} (green solid line), m_{a_1} (blue dashed line) and $m_{\tilde{\chi}_1^0}$ (brown dot-dashed line) on $\tan\beta$ for $M_1 = 120$ GeV, $M_2 = 200$ GeV, $\lambda = 0.55$ and $\kappa = 0.33$ with the other input parameters fixed to the values given in Table I.

both $\mu_{\rm eff}$ and $\tan\beta$, with m_{a_1} being comparatively more sensitive. Both these masses decrease with $\mu_{\rm eff}$. In case of NMSSM for large λ, where $\lambda \approx 0.5$–0.7, small values of $\tan\beta$ are preferred in order to obtain m_{h_1} in the desired mass window of 123–127 GeV. The mass of the lightest neutralino increases, as expected, with increasing $\mu_{\rm eff}$, and is almost independent of $\tan\beta$. Similarly, we can draw

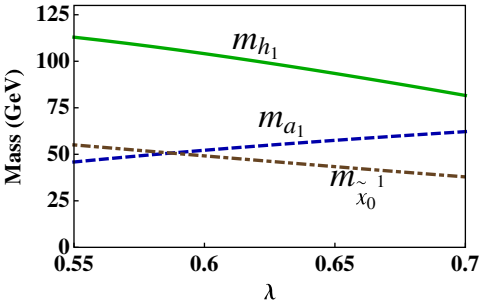

FIG. 6 (color online). Dependence of m_{h_1} (green solid line), m_{a_1} (blue dashed line) and $m_{\tilde{\chi}_1^0}$ (brown dot-dashed line) on λ for $M_1 = 120$ GeV, $M_2 = 200$ GeV and $\kappa = 0.33$ with the other input parameters fixed to the values given in Table I.

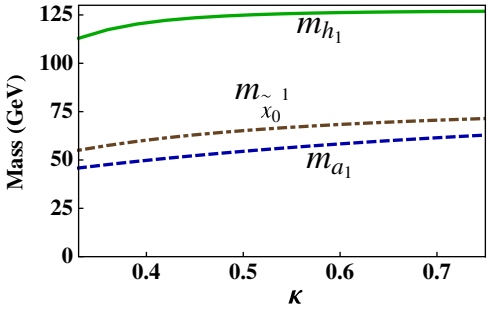

FIG. 7 (color online). Dependence of m_{h_1} (green solid line), m_{a_1} (blue dashed line) and $m_{\tilde{\chi}_1^0}$ (brown dot-dashed line) on κ for $M_1 = 120$ GeV, $M_2 = 200$ GeV and $\lambda = 0.55$ with the other input parameters fixed to the values given in Table I.

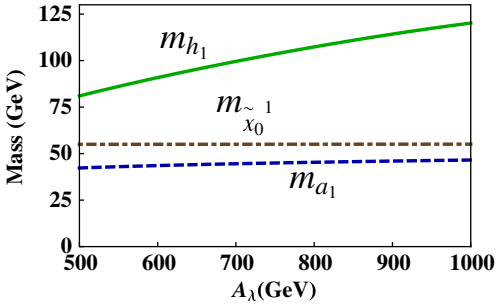

FIG. 8 (color online). Dependence of m_{h_1} (green solid line), m_{a_1} (blue dashed line) and $m_{\tilde{\chi}_1^0}$ (brown dot-dashed line) on A_λ for $M_1 = 120$ GeV, $M_2 = 200$ GeV, $\lambda = 0.55$ and $\kappa = 0.33$ with the other input parameters fixed to the values given in Table I.

conclusions from Figs. 6–9 regarding the dependence of the mass of the lightest scalar Higgs, lightest pseudoscalar Higgs and the lightest neutralino on different parameters of the NMSSM.

Before discussing the branching ratios of the lightest Higgs scalar to neutralinos and the lightest pseudoscalars, *with M_1 and M_2 treated as independent parameters*, in the

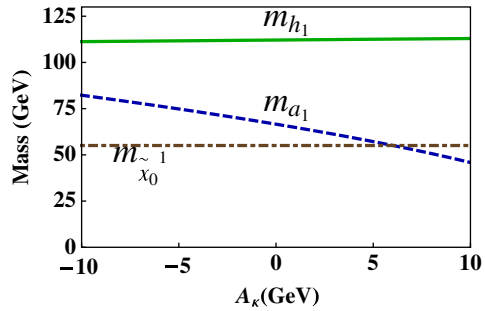

FIG. 9 (color online). Dependence of m_{h_1} (green solid line), m_{a_1} (blue dashed line) and $m_{\tilde{\chi}_1^0}$ (brown dot-dashed line) on A_κ for $M_1 = 120$ GeV, $M_2 = 200$ GeV, $\lambda = 0.55$ and $\kappa = 0.33$ with the other input parameters fixed to the values given in Table I.

following we summarize the dependence of our results on the various parameters of NMSSM:

(i) Dependence on M_1, M_2: If the value of M_1 is lowered below 30 GeV, the neutralino becomes sufficiently light, with $h_1 \to \tilde{\chi}_1^0\tilde{\chi}_1^0$ dominating over the decay $h_1 \to a_1 a_1$ for the entire parameter space considered here. If we decrease the value of M_2, the chargino mass bound from the LEP results in larger values of $\mu_{\rm eff}$ being disfavored.

(ii) Dependence on $\mu_{\rm eff}$: Increasing the value of the $\mu_{\rm eff}$, in the considered range, m_{a_1} reduces whereas $m_{\tilde{\chi}_1^0}$ increases. Therefore, the invisible branching ratio for $h_1 \to \tilde{\chi}_1^0\tilde{\chi}_1^0$ decreases, while the branching ratio of $h_1 \to a_1 a_1$ increases.

(iii) Dependence on $\tan\beta$: In this case, $h_1 \to \tilde{\chi}_1^0\tilde{\chi}_1^0$ decreases due to the increase of the branching ratio to lightest pseudoscalars, as the value of m_{a_1} decreases and $m_{\tilde{\chi}_1^0}$ remains constant.

(iv) Dependence on λ, κ: Increasing the value of λ increases the value of m_{a_1} and decreases $m_{\tilde{\chi}_1^0}$. Since λ also substantially affects the mass of m_{h_1}, other parameters need to be changed accordingly, so as to obtain the lightest CP-even Higgs h_1 in the required mass range. The dependence of $h_1 \to \tilde{\chi}_1^0\tilde{\chi}_1^0$ on λ and κ will be discussed in what follows.

(v) Dependence on A_λ, A_κ: The pseudoscalar and the neutralino mass is almost insensitive to A_λ. We have therefore performed our analyses for a fixed value of A_λ so as to have h_1 in the required mass range. The pseudoscalar mass is sensitive to A_κ, therefore the decay $h_1 \to a_1 a_1$ can be dominant for small $|A_\kappa|$.

We now consider the case when the soft gaugino masses are treated as independent parameters. In Fig. 10, we show contours of constant neutralino mass in the $\mu_{\rm eff} - M_1$ plane.

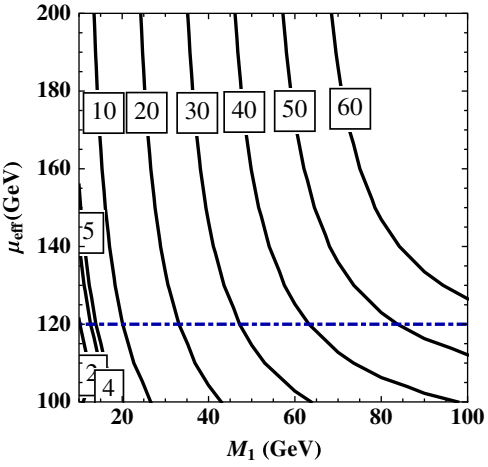

FIG. 10 (color online). Contours of constant lightest neutralino mass $m_{\tilde{\chi}_1^0}$ in the $\mu_{\rm eff} - M_1$ plane for $M_2 = 200$ GeV, $\lambda = 0.55$ and $\kappa = 0.6$ in NMSSM, with the other input parameters fixed at values as given in Table I.

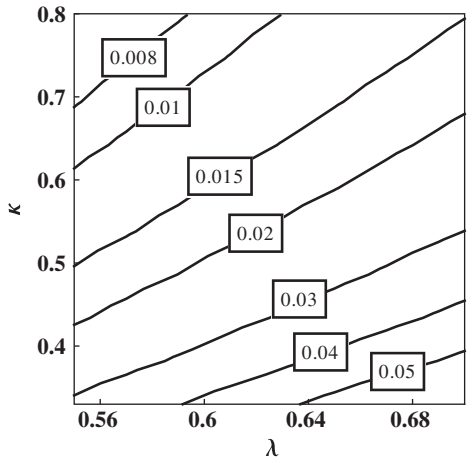

FIG. 11. Contours of the constant singlino composition for NMSSM in the $\kappa - \lambda$ plane for $M_2 = 200$ GeV and $M_1 = 5$ GeV, with the other input parameters fixed at values as in Table I.

We have taken into account the LEP constraint on the chargino mass ($m_{\tilde{\chi}^\pm} \geq 105$ GeV), as well as the invisible Z^0 decay width [Eq. (3.5)]. For the parameter space considered here, the Z^0 invisible decay width is less than 3 MeV. It can be seen from Fig. 10 that most of the parameter region with low M_1 allows a low-mass neutralino, making the Higgs invisible decay kinematically possible. The values in this figure are obtained with $\lambda = 0.55$ and $\kappa = 0.6$, with other parameter values as given in Table I, with $M_2 = 200$ GeV. The dependence of the constant contours on other parameters can be inferred from Figs. 5–9.

Before considering the invisible decay width, we show the contours of constant singlino component in the non-GUT scenario, with M_1 and M_2 treated as independent

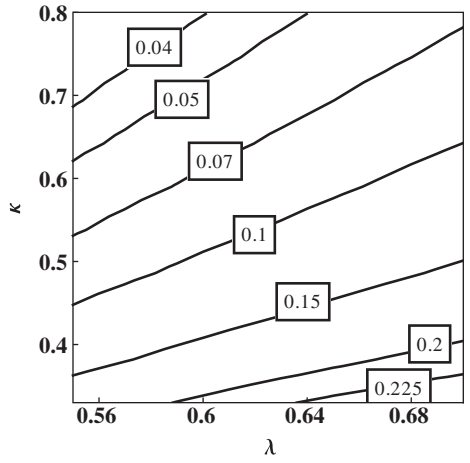

FIG. 12. Contours of constant singlino composition for NMSSM in the $\kappa - \lambda$ plane for $M_2 = 200$ GeV and $M_1 = 120$ GeV, with the other input parameters fixed at values as in Table I.

parameters. In Figs. 11 and 12, we show the constant singlino composition contours for two different values of $M_1 = 5$ GeV and 120 GeV, respectively, with a fixed value of $M_2 = 200$ GeV. The behavior of the constant contours can be understood from the fact that for low M_1, the neutralino is dominantly a gaugino type, with small singlino composition. Therefore, as discussed earlier, due to the small singlino composition, the invisible decay width of h_1 will be large compared to the GUT case. This can be seen in Fig. 13, where we show the invisible branching ratio of the Higgs decay to the lightest neutralinos in the $\mu_{\rm eff} - M_1$ plane. We have fixed $M_2 = 200$ GeV, $\lambda = 0.55$, $\kappa = 0.6$, with other input parameters as given in Table I. The LEP constraint on the chargino mass excludes the parameter region below $\mu_{\rm eff} = 120$ GeV, for $M_2 = 200$ GeV and is shown by the blue dot-dashed line. This limit on $\mu_{\rm eff}$ will decrease, with the increase in the value of M_2. The invisible decay width of the Z^0 to the lightest neutralinos satisfies the experimental constraints for the entire $\mu_{\rm eff} - M_1$ plane considered here. We see that in the allowed parameter space, the invisible branching ratio can be as large as 70%. The shape of the contours can be understood from Fig. 4, where we see that m_{a_1} decreases and $m_{\tilde{\chi}_1^0}$ increases, with increasing $\mu_{\rm eff}$, leading to $h_1 \to a_1 a_1$ at high $\mu_{\rm eff}$. At low $\mu_{\rm eff}$ and M_1, $\tilde{\chi}_2^0$ is sufficiently light, therefore the decay $h_1 \to \tilde{\chi}_1^0 \tilde{\chi}_2^0$ is kinematically possible. This explains the kinks in the contours. The second-lightest neutralino $\tilde{\chi}_2^0$ is mostly a Higgsino, at low $\mu_{\rm eff}$ and M_1. The bino component increases, with the increase in value of M_1, for a fixed $\mu_{\rm eff}$. The dominant branching ratio is seen for values of M_1 in the range of 40–70 GeV, where $m_{\tilde{\chi}_1^0}$ in turn varies from 30–60 GeV. In the region excluded by the chargino mass bound, it is seen that the branching ratio of Higgs to neutralinos can reach around 90% for $M_1 > 70$ GeV and low $\mu_{\rm eff}$. This is mainly because in this parameter region both $m_{\tilde{\chi}_2^0} < (m_{h_1} - m_{\tilde{\chi}_1^0})$ and $m_{a_1} < m_{h_1}/2$. Thus, if the bound on invisible branching ratio is considered to be less than 30%, most of the region with $\mu_{\rm eff} < 170$ GeV and $M_1 < 80$ GeV is disfavored by the invisible Higgs decay.

In order to fully understand the dependence of the invisible branching ratio on other input parameters of the NMSSM, in Fig. 14 we show its behavior in the $\mu_{\rm eff} - \tan\beta$ plane for $M_2 = 200$ GeV, $M_1 = 60$ GeV, $\lambda = 0.55$ and $\kappa = 0.6$. The other input parameters are fixed at values in Table I. We have shown the result for $M_1 = 60$ GeV, as we see from Fig. 13, the dominant branching ratio is seen for values of M_1 in the region of 40–70 GeV. The area between the green dotted lines in Fig. 14 shows the parameter region, which allows h_1 to be in the allowed mass range 123–127 GeV. The blue dot-dashed line represents the chargino mass bound from the LEP. We see that in the constrained space, the invisible branching ratio can be as high as 90%. At small values of $\tan\beta (< 10)$, when the value of $\mu_{\rm eff}$ is increased, the invisible branching ratio decreases as $m_{\tilde{\chi}_1^0}$ increases. The invisible branching ratio is small for $\tan\beta > 10$ and low $\mu_{\rm eff}$, due to the opening of the decay channel $h_1 \to a_1 a_1$, as m_{a_1} decreases with $\tan\beta$. This can be seen from Fig. 5. Therefore, considering the bound on $h_1 \to \tilde{\chi}_1^0 \tilde{\chi}_1^0$ to be less than 30%, $\mu_{\rm eff} < 180$ GeV and $\tan\beta > 10$ is disfavored. When M_1 is less than 40 GeV, the channel $h_1 \to \tilde{\chi}_1^0 \tilde{\chi}_2^0$ is kinematically accessible for low values of $\mu_{\rm eff}$. The invisible branching ratio in this case being small, a large parameter region in the $\mu_{\rm eff} - \tan\beta$ plane is favored by the bound from LHC experiments.

The sensitivity of our results on the parameters λ and κ can be understood from the behavior of the invisible branching ratio in the $\kappa - \lambda$ plane. This behavior depends on the composition of the lightest neutralino and can be

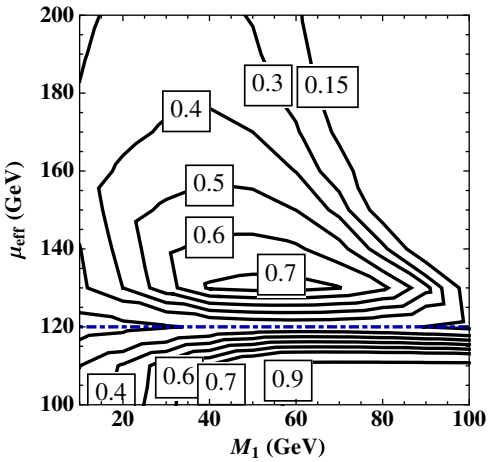

FIG. 13 (color online). Contours of constant branching ratio of $(h_1 \to \tilde{\chi}_1^0 \tilde{\chi}_1^0)$ in NMSSM in the $\mu_{\rm eff} - M_1$ plane for a fixed value of $M_2 = 200$ GeV, $\lambda = 0.55$ and $\kappa = 0.6$, with the other input parameters fixed at values as shown in Table I.

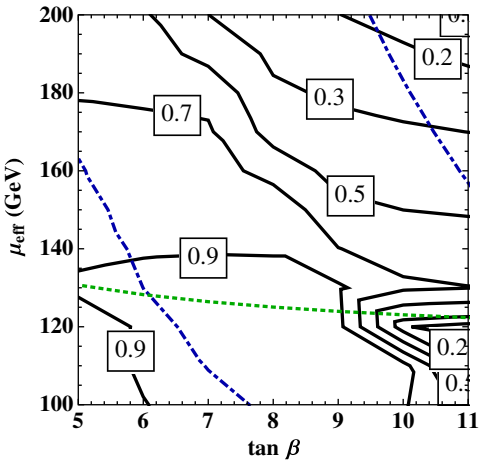

FIG. 14 (color online). Contours of constant branching ration of $(h_1 \to \tilde{\chi}_1^0 \tilde{\chi}_1^0)$ in the $\mu_{\rm eff} - \tan\beta$ plane for $M_2 = 200$ GeV, $M_1 = 60$ GeV, $\lambda = 0.55$ and $\kappa = 0.6$, with the other input parameters fixed at values as given in Table I. The area between the green dotted lines has h_1 in the mass range 123–127 GeV.

easily understood from Figs. 6 and 7. Since $m_{\tilde{\chi}_1^0}$ is sensitive to the gaugino mass parameter M_1, we discuss the behavior for different values of M_1. At low values of $M_1 < 30$ GeV, as discussed earlier, the channel $h_1 \to \tilde{\chi}_1^0\tilde{\chi}_2^0$ becomes kinematically accessible. Therefore, the Higgs invisible branching ratio is less than 30% for most of the $\kappa - \lambda$ parameter space. With $40 < M_1 < 70$ GeV, as can be seen from Fig. 13, the branching ratio of $h_1 \to \tilde{\chi}_1^0\tilde{\chi}_1^0$ is the largest. As $m_{\tilde{\chi}_1^0}$ decreases with λ (Fig. 6), the neutralino becomes light ($m_{\tilde{\chi}_1^0} < m_{h_1}/2$), and the mass of the lightest pseudoscalar Higgs increases ($m_{a_1} > m_{h_1}/2$), with $\lambda > 0.6$, even in case of large M_1. Therefore, the dominant decay mode is $h_1 \to \tilde{\chi}_1^0\tilde{\chi}_1^0$, with the branching ratio greater the 90% for $\lambda > 0.6$. This result is practically independent of κ, as can be seen from Fig. 7, where $m_{\tilde{\chi}_1^0}$, m_{a_1} is seen not to depend on κ. Again for large M_1 and $\lambda < 0.6$, with $m_{a_1} < m_{\tilde{\chi}_1^0}$, the branching ratio of $h_1 \to \tilde{\chi}_1^0\tilde{\chi}_1^0$ is smaller.

The invisible decay width mainly depends on the neutralino composition. The neutralino should have a small singlino component and a dominant bino component, i.e., M_1 should be small, in order to have a large invisible decay width. The decay width is also sensitive to the mass of the pseudoscalar Higgs a_1 and next-to-lightest neutralino $\tilde{\chi}_2^0$. The dependence of the width on the other input parameters $\tan\beta$, κ and λ is sensitive to the gaugino mass parameter M_1 and behaves differently for smaller and larger values of M_1. This is mainly because $m_{\tilde{\chi}_2^0}$ is also sensitive to M_1, leading to the opening of new decay channels.

V. SUMMARY AND CONCLUSIONS

We now summarize the results obtained in this work. We have considered the possibility of the invisible decays of the lightest CP-even Higgs boson in MSSM and in NMSSM. In the MSSM, we have considered both universal as well as nonuniversal gaugino masses at the GUT scale. In both cases we have seen that it is not possible to have a light neutralino, so that the decay of the lightest Higgs boson to lightest neutralinos does not take place. Our results show that in virtually all realistic scenarios, the nonuniversality is not sufficient to generate sufficiently light neutralinos. We have parametrized such nonuniversality in terms of a parameter r, which we have studied in detail. The details of such nonuniversality are briefly summarized in the Appendix.

We have then analyzed the possibility of having a light neutralino in the NMSSM extension of MSSM. We note that in the NMSSM, both the Higgs as well as the neutralino sectors are significantly richer, which provides us with greater possibilities. We have considered the neutralino sector of NMSSM, and in particular the phenomenon of the mixing of the singlino, and concluded that even in this case massless neutralinos cannot be realized with universal boundary conditions on the gaugino masses at the GUT scale, since the lightest Higgs is too heavy in conflict with the LHC result. Furthermore, with universal boundary conditions, the lightest Higgs $m_{h_1} \approx 126$ GeV would not decay to the lightest neutralinos. A related consideration is the ''ideal'' Higgs scenario motivated by LEP constraints, where the next-to-lightest CP-even Higgs h_2 can decay to lightest neutralinos. Departing from the assumption of universal gaugino masses, we have investigated the invisible branching ratio of the Higgs, as a function of the various parameters of NMSSM. We have concentrated on the case with the lightest scalar as the SM Higgs boson h_1, and have considered the dependence on parameters which are relevant to the Higgs and neutralino sector.

As is well known, the Higgs sector of the NMSSM itself is richer than the corresponding one in the MSSM. Thus, there is the intriguing possibility that the Higgs can decay into a pair of CP-odd lightest Higgs particles a_1. It is seen that for higher values of $\tan\beta$, the invisible branching ratio decreases, with the largest contribution coming from the Higgs decaying to two light pseudoscalar Higgs bosons. The present Higgs decay uncertainties can constrain NMSSM, but these constraints are strongly correlated with the composition of the lightest neutralino. The invisible branching ratio is found to be relatively independent of λ and κ, for 40 GeV $< M_1 <$ 60 GeV. In the NMSSM, the constraints on the Higgs mass results in small values of $\tan\beta$ being favored for large λ. We have discussed the dependence of our results on the parameters which enter the neutralino and the Higgs sectors of the NMSSM. From the dependence of the invisible branching ratio in the $\mu_{\text{eff}} - M_1$ plane, with other parameters fixed, we have shown that most of the parameter space is constrained by considering the invisible branching ratio $<30\%$. The dependence of this result on the other input parameters has also been discussed. For large values of $\tan\beta$, the invisible branching ratio decreases as a_1 becomes lighter, with $h_1 \to a_1 a_1$ kinematically possible. Therefore, at large $\tan\beta$, $M_1 < 40$ GeV is favored in the $\mu_{\text{eff}} - M_1$ plane, for all values of μ_{eff}. The allowed parameter region with $M_1 >$ 80 GeV remains unchanged. The sensitivity of the results on the input parameters λ, κ has also been discussed in detail. We have shown that for $M_1 < 70$ GeV, the results do not change significantly as a function of of λ and κ. But with large M_1 and $\lambda > 0.6$, the neutralinos become very light. In that case, the $\mu_{\text{eff}} - M_1$ parameter space is more tightly constrained. Further data from LHC may be able to shed light on the question of the invisible decays of the lightest Higgs boson.

ACKNOWLEDGMENTS

P. N. P. would like to thank the Centre for High Energy Physics, Indian Institute of Science, Bangalore for hospitality while this work was initiated, as well as the Inter-University Centre for Astronomy and Astrophysics, Pune, for hospitality where part of this work was done. The work of P. N. P. is supported by the J. C. Bose National

Fellowship of the Department of Science and Technology, India, and by the Council of Scientific and Industrial Research, India.

APPENDIX: NONUNIVERSAL GAUGINO MASSES IN GUTS

In this Appendix, we briefly discuss nonuniversal gaugino masses as they arise in grand unified models [67]. In grand unified supersymmetric models, nonuniversal gaugino masses are generated by a nonsinglet chiral superfield Φ^n that appears linearly in the gauge kinetic function $f(\Phi)$, which is an analytic function of the chiral superfields Φ in the theory [68]. The gaugino masses are generated from the coupling of the field strength superfield W^a with $f(\Phi)$, when the auxiliary part F_Φ of a chiral superfield Φ in $f(\Phi)$ gets a VEV. The Lagrangian for the coupling of gauge kinetic function to the gauge field strength can be written as

$$\mathcal{L}_{g.k.} = \int d^2\theta f_{ab}(\Phi) W^a W^b + \text{H.c.}, \tag{A1}$$

where a and b refer to gauge group indices, and repeated indices are summed over. The gauge kinetic function $f_{ab}(\Phi)$ is given by

$$f_{ab}(\Phi) = f_0(\Phi^s)\delta_{ab} + \sum_n f_n(\Phi^s)\frac{\Phi^n_{ab}}{M_P} + \cdots. \tag{A2}$$

Here Φ^s and the Φ^n are the singlet and the nonsinglet chiral superfields, respectively. Furthermore, $f_0(\Phi^s)$ and $f_n(\Phi^s)$ are functions of gauge singlet superfields Φ^s, and M_P denotes some large scale. When F_Φ gets a VEV $\langle F_\Phi \rangle$, the interaction in Eq. (A1) generates gaugino masses:

$$\mathcal{L}_{g.k.} \supset \frac{\langle F_\Phi \rangle_{ab}}{M_P}\lambda^a\lambda^b + \text{H.c.}, \tag{A3}$$

where $\lambda^{a,b}$ are gaugino fields. Here, we denote by λ^1, λ^2 and λ^3 the $U(1)$, $SU(2)$ and $SU(3)$ gaugino fields, respectively. Since the gauginos belong to the adjoint representation of the gauge group, Φ and F_Φ can belong to any of the representations appearing in the symmetric product of the two adjoint representations of unified gauge group.

TABLE IV. Ratios of the gaugino masses at the GUT scale in the normalization $M_1(\text{GUT}) = 1$, and at the electroweak scale in the normalization $M_1(\text{EW}) = 1$ for F terms in different representations of $SU(5)$. These results are obtained by using one-loop renormalization group equations.

$SU(5)$	M_1^G	M_2^G	M_3^G	M_1^{EW}	M_2^{EW}	M_3^{EW}
1	1	1	1	1	2	7.1
24	1	3	−2	1	6	−14.3
75	1	$-\frac{3}{5}$	$-\frac{1}{5}$	1	−1.18	−1.41
200	1	$\frac{1}{5}$	$\frac{1}{10}$	1	0.4	0.71

In the case where the SM gauge group is embedded within the grand unified gauge group $SU(5)$, for the symmetric product of the two adjoint (**24** dimensional) representations of $SU(5)$, we have

$$(\mathbf{24} \otimes \mathbf{24})_{\text{Symm}} = \mathbf{1} \oplus \mathbf{24} \oplus \mathbf{75} \oplus \mathbf{200}. \tag{A4}$$

In Table IV, we show the ratios of gaugino masses which result when F_Φ belongs to different representations of $SU(5)$ in the decomposition [Eq. (A4)].

Next we consider the embedding of the SM gauge group in a $SO(10)$ grand unified theory. The adjoint representation of $SO(10)$ being (**45**), Φ and F_Φ can belong to the symmetric product of two adjoint (**45**) dimensional representations [69]:

$$(\mathbf{45} \times \mathbf{45})_{\text{Symm}} = \mathbf{1} \oplus \mathbf{54} \oplus \mathbf{210} \oplus \mathbf{770}. \tag{A5}$$

In Table V we have shown the gaugino mass parameters for the different representations that arise in the symmetric product [Eq. (A5)] for the $SO(10)$ group. We note from Table V that the ratios of gaugino masses for the different representations of $SO(10)$ in the symmetric product [Eq. (A5)] with the unflipped embedding $SU(5) \subset SO(10)$ are identical to the corresponding gaugino mass ratios in Table IV for the embedding of SM in $SU(5)$. In case of the flipped embedding $SU(5)' \times U(1) \subset SO(10)$, as seen from Table VI, the gaugino mass ratios for the **210** and **770** dimensional representations of the grand unified gauge groups are different from the corresponding ratios for $SU(5)$. The ratio r, used for our analyses in Sec. II B, is obtained in this case from Tables V, VI, and VII, respectively.

Finally, we consider the grand unified group E_6, which has **78** as the adjoint representation [69]. The possible E_6 symmetric irreducible representations are

$$(\mathbf{78} \times \mathbf{78})_{\text{Symm}} = \mathbf{1} \oplus \mathbf{650} \oplus \mathbf{2430}. \tag{A6}$$

The corresponding quantities of interest for this case are tabulated in Tables VIII, IX, X, XI, XII, and XIII.

TABLE V. Ratios of the gaugino masses at the GUT scale in the normalization $M_1(\text{GUT}) = 1$, and at the electroweak scale in the normalization $M_1(\text{EW}) = 1$ for F terms in representations of $SU(5) \subset SO(10)$ with the normal (nonflipped) embedding. These results have been obtained at the one-loop level.

$SO(10)$	$SU(5)$	M_1^G	M_2^G	M_3^G	M_1^{EW}	M_2^{EW}	M_3^{EW}
1	**1**	1	1	1	1	2	7.1
54	**24**	1	3	−2	1	6	−14.3
210	**1**	1	1	1	1	2	7.1
	24	1	3	−2	1	6	−14.3
	75	1	$-\frac{3}{5}$	$-\frac{1}{5}$	1	−1.18	−1.41
770	**1**	1	1	1	1	2	7.1
	24	1	3	−2	1	6	−14.3
	75	1	$-\frac{3}{5}$	$-\frac{1}{5}$	1	−1.18	−1.14
	200	1	$\frac{1}{5}$	$\frac{1}{10}$	1	0.4	0.71

TABLE VI. Ratios of the gaugino masses at the GUT scale in the normalization $M_1(\mathrm{GUT}) = 1$, and at the electroweak scale in the normalization $M_1(\mathrm{EW}) = 1$ at the one-loop level for F terms in representations of flipped $SU(5)' \times U(1) \subset SO(10)$.

$SO(10)$	$[SU(5)' \times U(1)]_{\mathrm{flipped}}$	M_1^G	M_2^G	M_3^G	M_1^{EW}	M_2^{EW}	M_3^{EW}
1	(**1**, 0)	1	1	1	1	2	7.1
54	(**24**, 0)	1	3	−2	1	6	−14.3
210	(**1**, 0)	1	$-\frac{5}{19}$	$-\frac{5}{19}$	1	−0.52	−1.85
	(**24**, 0)	1	$-\frac{15}{7}$	$\frac{10}{7}$	1	−4.2	10
	(**75**, 0)	1	−15	−5	1	−28	−33.33
770	(**1**, 0)	1	$\frac{5}{77}$	$\frac{5}{77}$	1	0.13	0.46
	(**24**, 0)	1	$\frac{15}{101}$	$-\frac{10}{101}$	1	0.3	−0.70
	(**75**, 0)	1	−15	−5	1	−28	−33.3
	(**200**, 0)	1	5	$\frac{5}{2}$	1	9.33	16.67

TABLE VII. Ratios of the gaugino masses at the GUT scale in the normalization $M_1(\mathrm{GUT}) = 1$, and at the electroweak scale in the normalization $M_1(\mathrm{EW}) = 1$ at the one-loop level for F terms in representations of $SU(4) \times SU(2)_L \times SU(2)_R \subset SO(10)$.

$SO(10)$	$SU(4) \times SU(2)_R$	M_1^G	M_2^G	M_3^G	M_1^{EW}	M_2^{EW}	M_3^{EW}
1	(**1**, **1**)	1	1	1	1	2	7.1
54	(**1**, **1**)	1	3	2	1	6	−14.3
210	(**1**, **1**)	1	$-\frac{5}{3}$	0	1	−3.35	0
	(**15**, **1**)	1	0	$-\frac{5}{4}$	1	0	−9.09
	(**15**, **3**)	1	0	0	1	0	0
770	(**1**, **1**)	1	$\frac{25}{19}$	$\frac{10}{19}$	1	2.6	3.7
	(**1**, **5**)	1	0	0	1	0	0
	(**15**, **3**)	1	0	0	1	0	0
	(**84**, **1**)	1	0	$\frac{5}{32}$	1	0	1.11

TABLE VIII. Ratios of the gaugino masses at the GUT scale in the normalization $M_1(\mathrm{GUT}) = 1$, and at the electroweak scale in the normalization $M_1(\mathrm{EW}) = 1$ at the one-loop level for F terms in representations of $SU(5)'' \times U(1)' \times U(1) \subset [SO(10)' \times U(1)]_{\mathrm{flipped}} \subset E_6$.

E_6	$[SO(10)' \times U(1)]_{\mathrm{flipped}}$	$SU(5)''$	M_1^G	M_2^G	M_3^G	M_1^{EW}	M_2^{EW}	M_3^{EW}
1	(**1**, 0)	**1**	1	1	1	1	2	7.1
650	(**1**, 0)	**1**	1	$-\frac{5}{22}$	$-\frac{5}{22}$	1	−0.46	−1.61
	(**45**, 0)	**1**	1	0	0	1	0	0
		24	1	0	0	1	0	0
	(**54**, 0)	**24**	1	−15	10	1	−30	70
	(**210**, 0)	**1**	1	−5	−5	1	−10.0	−35.5
		24	1	$\frac{15}{2}$	−5	1	15.1	−35.5
		75	1	−15	−5	1	−30.1	−35.5
2430	(**1**, 0)	**1**	1	$\frac{5}{122}$	$\frac{5}{122}$	1	0.08	0.29
	(**45**, 0)	**1**	1	0	0	1	0	0
		24	1	0	0	1	0	0
	(**210**, 0)	**1**	1	−5	−5	1	−10.0	−35.5
		24	1	$\frac{15}{2}$	−5	1	15.1	−35.5
		75	1	−15	−5	1	−30.1	−35.5
	(**770**, 0)	**1**	1	1	1	1	2	7.1
		24	1	$-\frac{3}{5}$	$\frac{2}{5}$	1	−1.21	2.84
		75	1	−15	−5	1	−30.1	−35.5
		200	1	5	$\frac{5}{2}$	1	10.0	17.7

TABLE IX. Ratios of the gaugino masses at the GUT scale in the normalization $M_1(\mathrm{GUT}) = 1$, and at the electroweak scale in the normalization $M_1(\mathrm{EW}) = 1$ at the one-loop level for F terms in representations of $SU(4)' \times SU(2)_L \times SU(2)_X \times U(1) \subset [SO(10)' \times U(1)]_{\mathrm{flipped}} \subset E_6$.

E_6	$[SO(10)' \times U(1)]_{\mathrm{flipped}}$	$SU(4)'$	M_1^G	M_2^G	M_3^G	M_1^{EW}	M_2^{EW}	M_3^{EW}
1	(**1**, 0)	**1**	1	1	1	1	2	7.1
650	(**1**, 0)	**1**	1	$-\frac{5}{22}$	$-\frac{5}{22}$	1	−0.46	−1.61
	(**45**, 0)	**15**	1	0	0	1	0	0
	(**54**, 0)	**1**	1	−15	10	1	−30	70
	(**210**, 0)	**1**	0	1	0	0	1	0
		15	1	0	−5	1	0	−35.5
2430	(**1**, 0)	**1**	1	$\frac{5}{122}$	$\frac{5}{122}$	1	0.08	0.29
	(**45**, 0)	**15**	1	0	0	1	0	0
	(**210**, 0)	**1**	0	1	0	0	1	0
		15	1	0	−5	1	0	−35.5
	(**770**, 0)	**1**	1	25	10	1	50.2	70.9
		84	1	0	$\frac{5}{8}$	1	0	4.43

TABLE X. Ratios of the gaugino masses at the GUT scale in the normalization $M_1(\mathrm{GUT}) = 1$, and at the electroweak scale in the normalization $M_1(\mathrm{EW}) = 1$ at the one-loop level for F terms in representations of the trinification subgroup $SU(3)_C \times SU(3)_L \times SU(3)_R \subset E_6$.

E_6	$SU(3)_L \times SU(3)_R$	M_1^G	M_2^G	M_3^G	M_1^{EW}	M_2^{EW}	M_3^{EW}
1	(**1**, **1**)	1	1	1	1	2	7.1
650	$(\mathbf{1}, \mathbf{1})_1$	1	$-\frac{5}{3}$	0	1	−3.35	0
	$(\mathbf{1}, \mathbf{1})_2$	1	0	$-\frac{5}{4}$	1	0	−8.86
	(**1**, **8**)	1	0	0	1	0	0
	(**8**, **1**)	1	−5	0	1	−10.0	0
	(**8**, **8**)	1	0	0	1	0	0
2430	(**1**, **1**)	1	1	1	1	2	7.1
	(**1**, **8**)	1	0	0	1	0	0
	(**8**, **1**)	1	−5	0	1	−10.0	0
	(**8**, **8**)	1	0	0	1	0	0
	(**1**, **27**)	1	0	0	1	0	0
	(**27**, **1**)	1	$\frac{5}{9}$	0	1	1.12	0

TABLE XI. Ratios of the gaugino masses at the GUT scale in the normalization $M_1(\mathrm{GUT}) = 1$, and at the electroweak scale in the normalization $M_1(\mathrm{EW}) = 1$ at the one-loop level for F terms in representations of $SU(3)_C \times SU(3)_L \times U(1) \times SU(2)_X \subset SU(6) \times SU(2)_X \subset E_6$.

E_6	$SU(6) \times SU(2)_X$	$SU(3)_L$	M_1^G	M_2^G	M_3^G	M_1^{EW}	M_2^{EW}	M_3^{EW}
1	(**1**, **1**)	**1**	1	1	1	1	2	7.1
650	(**1**, **1**)	**1**	1	1	1	1	2	7.1
	(**35**, **1**)	**1**	1	5	−5	1	10.0	−35.5
		8	1	$\frac{5}{3}$	0	1	3.35	0
	(**189**, **1**)	**1**	1	$-\frac{1}{3}$	$-\frac{1}{3}$	1	−0.67	−2.36
		8	1	−1	0	1	−2	0
2430	(**1**, **1**)	**1**	1	1	1	1	2	7.1
	(**189**, **1**)	**1**	1	$-\frac{1}{3}$	$-\frac{1}{3}$	1	−0.67	−2.36
		8	1	−1	0	1	−2	0
	(**405**, **1**)	**1**	1	$\frac{5}{33}$	$\frac{5}{33}$	1	0.30	1.07
		8	1	$\frac{5}{19}$	0	1	0.53	0
		27	1	$\frac{5}{9}$	0	1	1.12	0

TABLE XII. Ratios of the gaugino masses at the GUT scale in the normalization $M_1(\mathrm{GUT}) = 1$, and at the electroweak scale in the normalization $M_1(\mathrm{EW}) = 1$ at the one-loop level for F terms in representations of $SU(3)_C \times SU(3)_L \times U(1) \times SU(2)_R \subset SU(6)' \times SU(2)_R \subset E_6$.

E_6	$SU(6)' \times SU(2)_R$	$SU(3)_L$	M_1^G	M_2^G	M_3^G	M_1^{EW}	M_2^{EW}	M_3^{EW}
1	(**1**, **1**)	**1**	1	1	1	1	2	7.1
650	(**1**, **1**)	**1**	1	$-\frac{5}{13}$	$-\frac{5}{13}$	1	−0.77	2.73
	(**35**, **1**)	**1**	1	5	−5	1	10.0	−35.5
		8	1	$-\frac{5}{3}$	0	1	3.35	0
	(**35**, **3**)	**1**	1	0	0	1	0	0
		8	1	0	0	1	0	0
	(**189**, **1**)	**1**	1	$-\frac{5}{3}$	$-\frac{5}{3}$	1	−3.35	−11.8
		8	1	5	0	1	10.0	0
2430	(**1**, **1**)	**1**	1	$\frac{15}{41}$	$\frac{15}{41}$	1	0.73	2.59
	(**1**, **5**)	**1**	1	0	0	1	0	0
	(**35**, **3**)	**1**	1	0	0	1	0	0
		8	1	0	0	1	0	0
	(**189**, **1**)	**1**	1	$-\frac{5}{3}$	$-\frac{5}{3}$	1	−3.35	−11.8
		8	1	5	0	1	10.0	0
	(**405**, **1**)	**1**	1	$\frac{5}{9}$	$\frac{5}{9}$	1	1.12	3.94
		8	1	$-\frac{5}{11}$	0	1	−0.91	0
		27	1	$\frac{5}{9}$	0	1	1.12	0

TABLE XIII. Ratios of the gaugino masses at the GUT scale in the normalization $M_1(\mathrm{GUT}) = 1$, and at the electroweak scale in the normalization $M_1(\mathrm{EW}) = 1$ at the one-loop level for F terms in representations of $SU(3)_C \times SU(3)_R \times U(1) \times SU(2)_L \subset SU(6)'' \times SU(2)_L \subset E_6$.

E_6	$SU(6)'' \times SU(2)_L$	$SU(3)_R$	M_1^G	M_2^G	M_3^G	M_1^{EW}	M_2^{EW}	M_3^{EW}
1	(**1**, **1**)	**1**	1	1	1	1	2	7.1
650	(**1**, **1**)	**1**	1	−5	1	1	−10.0	7.1
	(**35**, **1**)	**1**	1	0	$-\frac{5}{4}$	1	0	−8.86
	(**189**, **1**)	**1**	0	0	1	0	0	1
		8	1	0	0	1	0	0
2430	(**1**, **1**)	**1**	1	$\frac{35}{9}$	1	1	7.81	7.1
	(**189**, **1**)	**1**	0	0	1	0	0	1
		8	1	0	0	1	0	0
	(**405**, **1**)	**1**	1	0	$\frac{5}{12}$	1	0	2.95
		8	1	0	0	1	0	0
		27	1	0	0	1	0	0

[1] ATLAS Collaboration, Phys. Lett. B **716**, 1 (2012).
[2] ATLAS Collaboration, Report No. ATLAS-CONF-2013-014.
[3] CMS Collaboration, Phys. Lett. B **716**, 30 (2012).
[4] CMS Collaboration, arXiv:1303.4571.
[5] J. Ellis and T. You, arXiv:1303.3879.
[6] G. Belanger, B. Dumont, U. Ellwanger, J. F. Gunion, and S. Kraml, arXiv:1302.5694.
[7] J. R. Espinosa, M. Muhlleitner, C. Grojean, and M. Trott, J. High Energy Phys. 09 (2012) 126.
[8] J. R. Espinosa, C. Grojean, M. Muhlleitner, and M. Trott, J. High Energy Phys. 12 (2012) 045.
[9] P. P. Giardino, K. Kannike, M. Raidal, and A. Strumia, J. High Energy Phys. 06 (2012) 117.
[10] P. P. Giardino, K. Kannike, M. Raidal, and A. Strumia, Phys. Lett. B **718**, 469 (2012).
[11] Y. Bai, P. Draper, and J. Shelton, J. High Energy Phys. 07 (2012) 192.
[12] D. Ghosh, R. Godbole, M. Guchait, K. Mohan, and D. Sengupta, arXiv:1211.7015.
[13] H. K. Dreiner, J. S. Kim, and O. Lebedev, Phys. Lett. B **715**, 199 (2012).
[14] ATLAS Collaboration, Report No. ATLAS-CONF-2013-011.

[15] J. R. Forshaw, J. F. Gunion, L. Hodgkinson, A. Papaefstathiou, and A. D. Pilkington, J. High Energy Phys. 04 (2008) 090.
[16] M. Almarashi and S. Moretti, Phys. Rev. D **84**, 035009 (2011).
[17] G. Belanger, U. Ellwanger, J. F. Gunion, Y. Jiang, S. Kraml, and J. H. Schwarz, J. High Energy Phys. 01 (2013) 069.
[18] U. Ellwanger and C. Hugonie, Adv. High Energy Phys. **2012**, 625389 (2012).
[19] T. Gherghetta, B. von Harling, A. D. Medina, and M. A. Schmidt, J. High Energy Phys. 02 (2013) 032.
[20] S. F. King, M. Muhlleitner, R. Nevzorov, and K. Walz, Nucl. Phys. **B870**, 323 (2013).
[21] N. D. Christensen, T. Han, Z. Liu, and S. Su, arXiv:1303.2113.
[22] R. Barate *et al.* (LEP Working Group for Higgs Boson Searches and ALEPH, DELPHI, L3, and OPAL Collaborations), Phys. Lett. B **565**, 61 (2003).
[23] I. Gogoladze, J. D. Lykken, C. Macesanu, and S. Nandi, Phys. Rev. D **68**, 073004 (2003).
[24] D. Choudhury, H. K. Dreiner, P. Richardson, and S. Sarkar, Phys. Rev. D **61**, 095009 (2000).
[25] H. K. Dreiner, C. Hanhart, U. Langenfeld, and D. R. Phillips, Phys. Rev. D **68**, 055004 (2003).
[26] H. K. Dreiner, M. Hanussek, J. S. Kim, and S. Sarkar, Phys. Rev. D **85**, 065027 (2012).
[27] H. K. Dreiner, S. Heinemeyer, O. Kittel, U. Langenfeld, A. M. Weber, and G. Weiglein, Eur. Phys. J. C **62**, 547 (2009).
[28] A. Bartl, H. Fraas, W. Majerotto, and N. Oshimo, Phys. Rev. D **40**, 1594 (1989).
[29] H. E. Haber and G. L. Kane, Phys. Rep. **117**, 75 (1985).
[30] S. Schael *et al.* (ALEPH, DELPHI, L3, OPAL, and SLD Collaborations, LEP Electroweak Working Group, SLD Electroweak Group, and SLD Heavy Flavour Group), Phys. Rep. **427**, 257 (2006).
[31] S. P. Martin and P. Ramond, Phys. Rev. D **48**, 5365 (1993).
[32] P. Ramond, arXiv:hep-ph/9809459.
[33] K. Griest and H. E. Haber, Phys. Rev. D **37**, 719 (1988).
[34] G. Bertone, D. Hooper, and J. Silk, Phys. Rep. **405**, 279 (2005).
[35] S. Heinemeyer, W. Hollik, A. M. Weber, and G. Weiglein, J. High Energy Phys. 04 (2008) 039.
[36] A. Belyaev, N. D. Christensen, and A. Pukhov, Comput. Phys. Commun. **184**, 1729 (2013).
[37] ATLAS Collaboration, Report No. ATLAS-CONF-2012-033.
[38] CMS Collaboration, Report No. CMS-PAS-SUS-12-005.
[39] P. Fayet, Nucl. Phys. **B90**, 104 (1975); H. P. Nilles, M. Srednicki, and D. Wyler, Phys. Lett. **120B**, 346 (1983).
[40] J. R. Ellis, J. F. Gunion, H. E. Haber, L. Roszkowski, and F. Zwirner, Phys. Rev. D **39**, 844 (1989).
[41] M. Drees, Int. J. Mod. Phys. A **04**, 3635 (1989).
[42] P. N. Pandita, Phys. Lett. B **318**, 338 (1993).
[43] P. N. Pandita, Z. Phys. C **59**, 575 (1993).
[44] U. Ellwanger, Phys. Lett. B **303**, 271 (1993).
[45] T. Elliott, S. F. King, and P. L. White, Phys. Lett. B **314**, 56 (1993).
[46] P. N. Pandita, Phys. Rev. D **50**, 571 (1994).
[47] P. N. Pandita, Z. Phys. C **63**, 659 (1994).
[48] S. Y. Choi, D. J. Miller, and P. M. Zerwas, Nucl. Phys. **B711**, 83 (2005).
[49] J. Cao and J. M. Yang, Phys. Rev. D **78**, 115001 (2008).
[50] U. Ellwanger, J. F. Gunion, and C. Hugonie, J. High Energy Phys. 02 (2005) 066.
[51] U. Ellwanger and C. Hugonie, Comput. Phys. Commun. **175**, 290 (2006).
[52] F. Franke and H. Fraas, Int. J. Mod. Phys. A **12**, 479 (1997).
[53] F. Franke and H. Fraas, Z. Phys. C **72**, 309 (1996).
[54] G. Belanger, F. Boudjema, C. Hugonie, A. Pukhov, and A. Semenov, J. Cosmol. Astropart. Phys. 09 (2005) 001.
[55] G. Belanger, F. Boudjema, A. Pukhov, and A. Semenov, Comput. Phys. Commun. **176**, 367 (2007).
[56] C. Bennett *et al.* (WMAP Collaboration), Astrophys. J. Suppl. Ser. **148**, 97 (2003); D. N. Spergel *et al.* (WMAP Collaboration), Astrophys. J. Suppl. Ser. **148**, 175 (2003).
[57] R. Dermisek and J. F. Gunion, Phys. Rev. D **73**, 111701 (2006).
[58] R. Dermisek and J. F. Gunion, Phys. Rev. D **79**, 055014 (2009).
[59] R. Dermisek and J. F. Gunion, Phys. Rev. D **81**, 075003 (2010).
[60] G. Calderini, EPJ Web Conf. **28**, 04005 (2012).
[61] C. Englert, M. Spannowsky, and C. Wymant, Phys. Lett. B **718**, 538 (2012).
[62] D. G. Cerdeno, P. Ghosh, and C. B. Park, arXiv:1301.1325.
[63] J. P. Lees *et al.* (*BABAR* Collaboration), Phys. Rev. D **87**, 031102(R) (2013).
[64] J. Rorie (on behalf of the Belle Collaboration), Proc. Sci., EPSHEP2011 (2011) 257.
[65] CMS Collaboration, Phys. Rev. Lett. **109**, 121801 (2012).
[66] CMS Collaboration, arXiv:1210.7619.
[67] P. N. Pandita and M. Patra, Int. J. Mod. Phys. A **27**, 1250172 (2012).
[68] E. Cremmer, S. Ferrara, L. Girardello, and A. Van Proeyen, Phys. Lett. B **116**, 231 (1982).
[69] S. P. Martin, Phys. Rev. D **79**, 095019 (2009).